



## Impact Characterisation of Glass Fibre-Reinforced Polymer (GFRP) Type C-600 and E-800 Using a Single Stage Gas Gun (SSGG)

Syafiqah Nur Azrie, S., Mohamed Thariq, H. S.\* and Francisco, C.

*Aerospace Manufacturing Research Centre, Faculty of Engineering, Universiti Putra Malaysia, 43400 UPM, Serdang, Selangor, Malaysia*

### ABSTRACT

This paper presents experimental findings derived from high velocity impact tests on woven-roving Glass Fibre-Reinforced Polymers (GFRP) Type E-800 g/m<sup>2</sup> and Type C-600 g/m<sup>2</sup>. The effects on specimen thickness, projectile shape and gas gun pressure were investigated. As the gas gun pressure increases, there is a proportional increase in the projectile kinetic energy, the projectile initial velocity, the maximum force exerted on the specimens and in energy absorption upon impact. During the test, the shape of the projectile, the target thickness and the gas gun pressure significantly affected the impact performance of the GFRP. From the experiment, it was found that GFRP Type E-800 g/m<sup>2</sup> is stronger and more impact resistant compared with GFRP Type C-600 g/m<sup>2</sup>, due to the fact that E-glass materials have higher fibre volume and density and overall better mechanical properties than C-glass fibres. Therefore, GFRP Type E-800 g/m<sup>2</sup> composites should be considered for applications in load and impact bearing aircraft structures.

*Keywords:* Energy Absorption, Glass Fiber Reinforced Polymer (GFRP), High Velocity Impact (HVI), Impact Characterisation, Polymer Matrix Composites (PMC), Single Stage Gas Gun (SSGG)

### INTRODUCTION

Polymer matrix composites (PMCs) in the form of Glass Fibre-Reinforced Polymers (GFRPs) is extensively used in engineering structures. It is usually applied in the aviation industry due to their properties, such as stiffness, high strength and great fatigue resistance. It is also the most economical choice in terms of manufacturing life cycle costs. Currently, in military applications, there has been an increasing demand to reduce the weight of armour structures, which will improve the armoured vehicle mobility, fuel efficiency and transportability and thus GFRPs are good a choice as they can resist heavy loads and offer great resistance to impact.

#### *Article history:*

Received: 08 January 2016

Accepted: 11 November 2016

#### *E-mail addresses:*

[snasafri@gmail.com](mailto:snasafri@gmail.com) (Syafiqah Nur Azrie, S.),

[thariq@upm.edu.my](mailto:thariq@upm.edu.my) (Mohamed Thariq, H. S.),

[francisco.c@upm.edu.my](mailto:francisco.c@upm.edu.my) (Francisco, C.)

\*Corresponding Author

Impact loading are divided into the following categories: low, intermediate, high/ballistic and hyper velocity impact. Naik and Shirao (2004) state that as the projectile velocity varies, there are distinct differences in damage propagations, energy transfer and energy dissipation between the target and the impacting projectile. Vaidya (2011), shows that hyper impacts occur between 2 km/s and 5 km/s, high ballistic impacts within the range of 50 m/s and 1000 m/s, intermediate is between 10 m/s and 50 m/s while low velocity impacts occur at 10 m/s.

According to Zhou (1995), Davies (1996) and Belingardi and Vadori (2002), GFRPs have higher impact damage tolerance than carbon fibre-based laminates in addition to being cheaper. Bibo and Hogg (1998) and Thanomsilp and Hogg (2003) said that GFRP laminates have greater impact resistance since they have higher energy absorption due to their higher strain to failure ratio compared with carbon fibre-reinforced composites.

The GFRPs have lower Young's modulus and density but a higher strength compared with carbon fibre laminates. The GFRP Type E fibres are commonly used in structural applications but they experience degradation in highly acidic or alkaline environment. Therefore, resistant glass was developed such as C-glass, also known as 'chemical' glass. Type C-glass is used as a surface coating in water pipes and tanks. Table 1 shows the mechanical properties of GFRP Type C and Type E, confirming that the tensile strength, density and modulus of elasticity of GFRP Type C are lower than those of GFRP Type E (Hausrath & Longobardo, 2010).

Table 1  
*Mechanical Properties of GFRP Type E and Type C (Hausrath & Longobardo, 2010)*

Property	E-glass	C-glass
Tensile strength at 23°C (MPa)	3445	3310
Elongation percentage	4.8	4.8
Young's modulus at 23°C (GPa)	72.3	68.9
Density (g/cm <sup>3</sup> )	2.58	2.52

Type C-glass fibre with a mass of 600 g/m<sup>2</sup> is thinner compared with Type E-glass fibre with a mass of 800 g/m<sup>2</sup>. The hardness of Type E fibre with a mass of 800 g/m<sup>2</sup> is higher than the value for Type C fibre with a mass of 600 g/m<sup>2</sup> since its fibre composition is greater. There are only a few studies that evaluated the performance of Type E-800 g/m<sup>2</sup> and Type C-glass/Epoxy 600g/m<sup>2</sup> composite materials.

### Factors Influencing Impact Characteristic

**Influence of fibre properties.** Naik and Shirao (2004) compared twill weave T300 carbon/epoxy composite and two-dimensional woven fabric of plain weave E-glass/epoxy to study their ballistic impact behaviour. The results indicated that E-glass/epoxy panels have higher ballistic limit than T300 carbon/epoxy laminates.

**Influence of Specimen Thickness.** Naik and Doshi (2008) report that during high velocity impact test, thickness of the composite materials is a significant performance factor. Gellert,

Cimpoeru and Woodward (2000) discovered that energy absorption during impact in thin Glass Reinforced Polymer (GRP) is independent of the projectile nose geometry. This study focused on three different projectile shapes and the perforation of GRP composites. Shaktivesh, Nair, Sesha Kumar and Naik (2013) studied the effect of panel thickness on the impact damage and found that energy absorbed by various mechanisms increases and is directly proportional to the target thickness and the velocity of the projectile.

**Influence of Projectile Shape and mass.** Projectile shapes normally tested in high velocity impact experiment are blunt, conical, or hemispherical. Corran, Shadbolt and Ruiz (1983) found that the projectile nose radius affects critical impact energy. Børvik et al. (2002) report that hemispherical projectiles affect tensile stretching after severe indentation and thinning of the specimen, while conical shape projectiles affect ductile hole expansion in thicker specimens and peeling in thinner specimens. Blunt projectiles affect failure through shear plugging. Ohte, Yoshizawa, Chiba and Shida (1982) compared three different shapes of projectile and have established that the conical projectiles required less perforation energy to penetrate the target. Wen (2000) and Wen (2001) came up with model to estimate the penetration and perforation of monolithic composite laminates impacted transversely by projectiles with different nose shapes.

**Influence of Projectile Velocity.** In high velocity impact testing, gas driven guns that uses high pressure can determine projectile velocity . Previous research has usually involved experiments on the impact parameter effects that affect the impact test result. Very limited research has been carried out to compare impact resistance of different types of composite materials.

Therefore, seeks to evaluate and understand the differences in impact response between Glass Fibre Reinforced Polymer (GFRP) Type C-600 g/m<sup>2</sup> and Type E-800 g/m<sup>2</sup> since both of these materials are potentially useful in aircraft applications. This research compares the impact response of Glass Fibre Reinforced Polymer (GFRP) Type C-600 g/m<sup>2</sup> and Type E-800 g/m<sup>2</sup> using high velocity impact testing and investigates specimen thickness, type of projectiles, and projectile velocity on the impact characteristics of these two types of glass-fibre reinforced composite materials.

## METHODOLOGY

### Specimen Preparation

The specimen was prepared at the Aerospace Material Laboratory, Faculty of Engineering, Universiti Putra Malaysia. The matrix solution is based on a 2:1 ratio portions of epoxy to the hardener. The epoxy and hardener are Zeepoxy HL002TA and Zeepoxy HL002TB respectively. The specimens were fabricated using a hot bonder machine, as previously reported by Ilcewicz et al. (Ilcewicz, Cheng, Hafenricher & Seaton, 2009). For Glass Fibre Reinforced Polymer (GFRP) Type E-800 g/m<sup>2</sup> and Type C-600 g/m<sup>2</sup>, the temperature applied was 150°F and the composite panels were hold at this temperature for 120 minutes to obtain fully cured GFRP laminates.

A hot bonder is a portable device that controls heating based on temperature feedback from the area under repair. The cure cycle is controlled using thermocouples and data can be printed out. The hot bonder machine is used together with vacuum bagging. This technique can hold

the resin in place until it fully cures using atmospheric pressure as reported by Ilcewicz et al. (2009) and Petrone et al. (2014). The high velocity impact test specimens were then cut, using a CNC Router Machine, ACM 1325, to a size of 100 mm × 100 mm (Hameed Sultan, 2007).

The stacking sequence of the glass fibre was set at 0°. Glass Fibre Reinforced Polymer (GFRP) Type E-800 g/m<sup>2</sup> and Type C-600 g/m<sup>2</sup> were fabricated into four different thicknesses, 6 mm, 8 mm, 10 mm and 12 mm, as shown in Table 2.

Table 2

*Number of plies used in the laminates with Type E-glass/epoxy 800 g/m<sup>2</sup> and Type C-glass/epoxy 600 g/m<sup>2</sup> for the high velocity impact tests*

Type of GFRP	Thickness, (mm)	Number of plies
E-glass/Epoxy 800 g/m <sup>2</sup>	6	9
	8	12
	10	15
	12	18
C-glass/Epoxy 600 g/m <sup>2</sup>	6	9
	8	12
	10	15
	12	17

### Experimental Setup

High energy impact tests were carried out using a single stage gas gun (SSGG) at the Faculty of Manufacturing Engineering, Universiti Malaysia Pahang. In this test, specimens with dimension of 100 mm × 100 mm were impacted with three types of projectiles: blunt, conical and hemispherical. The speed of the projectiles during the test was set up and varied using the pressure control of the gas gun. In this test, the projectile velocity range is within 70-240 m/s.

The gas gun uses compressed helium gas to fire the projectile. The velocity of the projectile is controlled by the gas pressure. Three samples for each testing condition are used to obtain average values and standard deviation values. The gas gun is connected to a ballistic data acquisition system. The software performs its calculations from the basic force-time information including projectile velocity, maximum force, kinetic energy and energy absorbed by the impacted specimen.

### Impact Mechanics

In high velocity impact testing, the varying parameters are the gas gun pressure which will affect the projectile initial velocity, the target thickness and the projectile shape. The high velocity impact testing uses the single stage gas gun, which is connected to the ballistic data acquisition system. Data obtained from the system are: maximum force, kinetic energy, approximate projectile speed and absorbed energy. The approximate projectile velocity and the maximum force are obtained from the force transducer in the catch chamber. The projectile kinetic energy can be obtained from the kinetic energy, KE equation of a non-rotating object of mass, m, travelling at a speed, v:

$$KE = \frac{1}{2} mv^2 \quad [1]$$

The mass value is the projectile mass (in grams) while the velocity value refers to the projectile velocity in ms<sup>-1</sup>. The absorbed energy value can be obtained applying the (2). The work done by a constant force of magnitude, F, on a point that moves a displacement (not distance), s, in the direction of the force is the product as given in (2):

$$\text{Energy Absorbed} = F \times s \quad [2]$$

In this test, the force value, F, is obtained from the force sensor installed in the single stage gas gun (SSGG). The displacement value, s, is the horizontal distance a projectile travels from the nozzle to the specimen which is also equal to the distance from the nozzle to the specimen. Table 3 shows the pressure applied during the tests for both GFRP laminates. Three specimens will be tested for each test, to check the repeatability of the experimental results.

Table 3

*Pressure tested for both GFRP laminates with each shape of projectile*

Thickness	Pressure (bar)							
	8	12	15	16	20	25	30	40
6 mm	///	///		///				
8 mm			///		///	///		
10 mm					///		///	///
12 mm					///		///	///

\* / indicates number of test

### Material Properties of the Projectile – Mild Steel

There are three classes of projectiles: soft projectiles, semi-hard projectiles and hard projectiles. A soft projectile is the type that will experience clear deformation during impact. Grytten et al. (2009) state that a semi-hard projectile will have some deformation during the impact test, while hard projectiles undergo little or negligible deformation. The projectiles used in this experiment are made of mild steel with low hardness to avoid erosion inside the surface of the barrel. Mild steel containing a slight fraction of carbon is tough but not really hard. In this experiment, three different types of projectile are used, e.g. blunt, conical and hemispherical as shown in Figure 1.

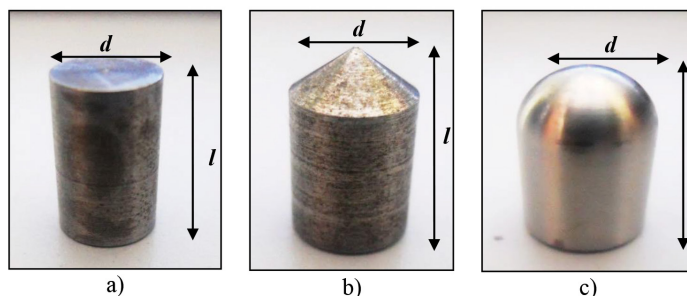


Figure 1. Types of projectile used in the actual impact testing a) blunt b) conical c) hemispherical

Table 4 shows the dimensions of the projectiles used in this experiment. Even though the dimension of these projectiles is the same, the mass is different. The differences in mass and shape of the projectile significantly affect its velocity during the impact test.

Table 4  
Dimensions of projectile

Type	Length, <i>l</i> (mm)	Diameter, <i>d</i> (mm)	Mass (g)
Blunt	15	10	6
Conical	15	10	5
Hemispherical	15	10	5

## RESULTS AND DISCUSSIONS

The high velocity impact test results using a Single Stage Gas Gun (SSGG) for both materials, GFRP Type E-800 g/m<sup>2</sup> and Type C-glass/Epoxy 600g/m<sup>2</sup>, are presented in this section. Target plates of four different thicknesses were impacted at varying velocities by projectiles of different nose shape. For each thickness, three different gas gun pressures were used. A pilot high velocity impact test was conducted to identify the maximum gas gun pressure that can be applied before penetration occurs for each thickness value of the panels. Thus, the three best pressures were decided to test for each one of the four panels with different thickness.

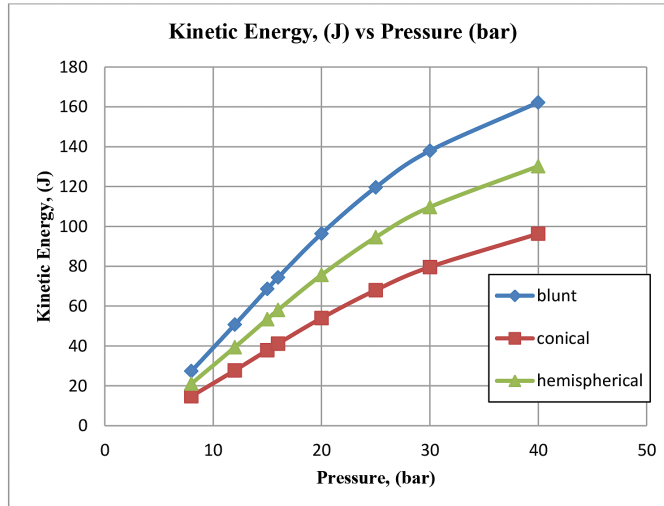
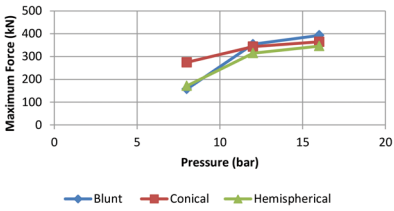
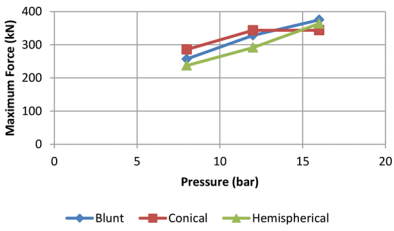
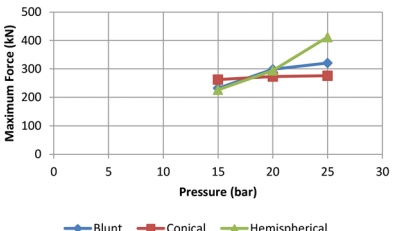
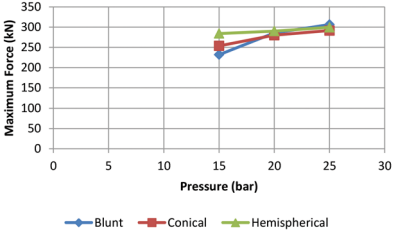
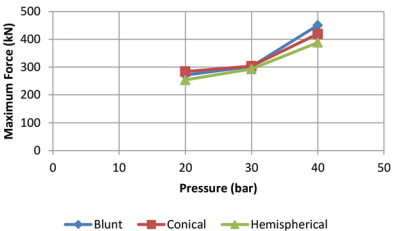


Figure 2. Kinetic Energy-Pressure curve for blunt, conical and hemispherical shapes of projectiles

Figure 2 shows the projectile kinetic energy and pressure curves for the three different projectiles experimented in this research. It shows that as the gas gun pressure increases, the projectile kinetic energy also increases. The blunt projectile has the highest kinetic energy for all tested gas pressures because the kinetic energy of a projectile is proportional to its mass and velocity. Since the mass of the blunt projectile is higher than the mass of the hemispherical and

conical projectiles, it therefore has the highest kinetic energy of all the projectiles as shown in Figure 2. Even though the hemispherical and conical projectiles have the same mass, the shape of the projectiles are different which affects their kinetic energy.

### Impact Force Analysis

Type C-600 g/m <sup>2</sup>	<p style="text-align: center;"><b>6 mm</b></p>  <p style="text-align: center;">Maximum Force (kN)</p> <p style="text-align: center;">Pressure (bar)</p> <p style="text-align: center;">—●— Blunt —■— Conical —▲— Hemispherical</p>
Type E-800 g/m <sup>2</sup>	<p style="text-align: center;"><b>6 mm</b></p>  <p style="text-align: center;">Maximum Force (kN)</p> <p style="text-align: center;">Pressure (bar)</p> <p style="text-align: center;">—●— Blunt —■— Conical —▲— Hemispherical</p>
Type C-600 g/m <sup>2</sup>	<p style="text-align: center;"><b>8 mm</b></p>  <p style="text-align: center;">Maximum Force (kN)</p> <p style="text-align: center;">Pressure (bar)</p> <p style="text-align: center;">—●— Blunt —■— Conical —▲— Hemispherical</p>
Type E-800 g/m <sup>2</sup>	<p style="text-align: center;"><b>8 mm</b></p>  <p style="text-align: center;">Maximum Force (kN)</p> <p style="text-align: center;">Pressure (bar)</p> <p style="text-align: center;">—●— Blunt —■— Conical —▲— Hemispherical</p>
Type C-600 g/m <sup>2</sup>	<p style="text-align: center;"><b>10 mm</b></p>  <p style="text-align: center;">Maximum Force (kN)</p> <p style="text-align: center;">Pressure (bar)</p> <p style="text-align: center;">—●— Blunt —■— Conical —▲— Hemispherical</p>

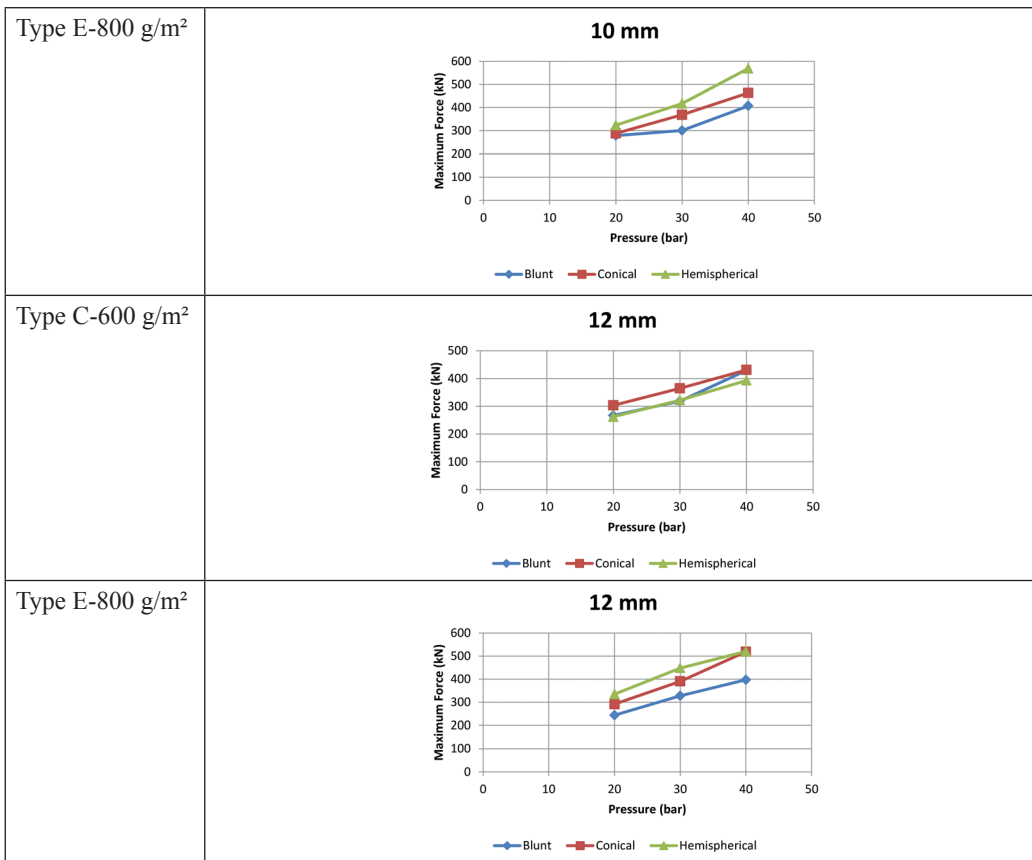


Figure 3. Maximum Force-Pressure curve for 6 mm, 8 mm, 10 mm, 12 mm thickness for Type C-glass/epoxy 600 g/m<sup>2</sup> and Type E-glass/epoxy 800 g/m<sup>2</sup>

Figure 3 shows the relationship between maximum force and pressure for Type C-600 g/m<sup>2</sup> and Type E-800 g/m<sup>2</sup> composites for each of the panel thickness, 6 mm, 8 mm, 10 mm, and 12 mm. As the pressure increases, the maximum force exerted on the specimen also increases. This is because the projectile velocity increases with the pressure in the gas gun, and as a result, the maximum force exerted on the specimen also increases. Due to the different shape of the projectile the contact area between the composite and the impactor changes, affecting the force exerted onto the specimen.

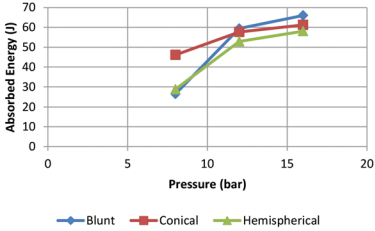
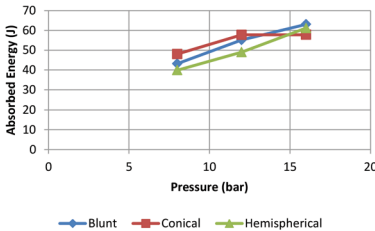
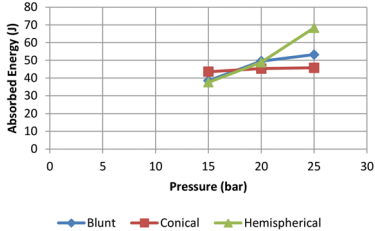
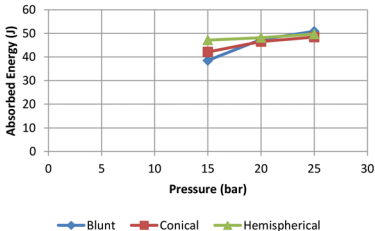
From Figure 3, it can be observed that the conical projectile provides the highest maximum force followed by the hemispherical and blunt projectiles respectively. This is because the shape of the conical projectile means that it has the smallest contact area compared with the other two projectiles. Therefore, the contact area between the projectile and the tested specimen affect the maximum force exerted on the specimen during the impact. The forces acting on the projectile are the summation of the inertial force and the compressive force.

Inertial force depends on the velocity and the projectile cross sectional area, target density and shape of projectile. Awerbuch and Bodner (1974) found that inertial force is also known as work done, which can be obtained by equating the initial force on the target to the change in



the kinetic energy of the material. The compressive force is the product of compressive stress at the tip of the projectile and the cross-sectional area of the projectile. According to Udatha et al. (2012), compressive force is obtained using an interactive approach starting with a trial value of the compressive stress at the tip of the projectile. Mili (2012) says initial total contact force is the summation of inertial force and the compressive force and the impact force and central deflection are proportional to the projectile velocity.

### Energy Absorbed Analysis

Type C-600 g/m <sup>2</sup>	<p style="text-align: center;"><b>6 mm</b></p>  <table border="1" style="margin-left: auto; margin-right: auto;"> <caption>Data for Type C-600 g/m<sup>2</sup> (6 mm)</caption> <thead> <tr> <th>Pressure (bar)</th> <th>Blunt (J)</th> <th>Conical (J)</th> <th>Hemispherical (J)</th> </tr> </thead> <tbody> <tr> <td>8</td> <td>30</td> <td>45</td> <td>28</td> </tr> <tr> <td>12</td> <td>58</td> <td>58</td> <td>52</td> </tr> <tr> <td>16</td> <td>68</td> <td>62</td> <td>58</td> </tr> </tbody> </table>	Pressure (bar)	Blunt (J)	Conical (J)	Hemispherical (J)	8	30	45	28	12	58	58	52	16	68	62	58
Pressure (bar)	Blunt (J)	Conical (J)	Hemispherical (J)														
8	30	45	28														
12	58	58	52														
16	68	62	58														
Type E-800 g/m <sup>2</sup>	<p style="text-align: center;"><b>6 mm</b></p>  <table border="1" style="margin-left: auto; margin-right: auto;"> <caption>Data for Type E-800 g/m<sup>2</sup> (6 mm)</caption> <thead> <tr> <th>Pressure (bar)</th> <th>Blunt (J)</th> <th>Conical (J)</th> <th>Hemispherical (J)</th> </tr> </thead> <tbody> <tr> <td>8</td> <td>42</td> <td>48</td> <td>38</td> </tr> <tr> <td>12</td> <td>58</td> <td>58</td> <td>48</td> </tr> <tr> <td>16</td> <td>65</td> <td>58</td> <td>58</td> </tr> </tbody> </table>	Pressure (bar)	Blunt (J)	Conical (J)	Hemispherical (J)	8	42	48	38	12	58	58	48	16	65	58	58
Pressure (bar)	Blunt (J)	Conical (J)	Hemispherical (J)														
8	42	48	38														
12	58	58	48														
16	65	58	58														
Type C-600 g/m <sup>2</sup>	<p style="text-align: center;"><b>8 mm</b></p>  <table border="1" style="margin-left: auto; margin-right: auto;"> <caption>Data for Type C-600 g/m<sup>2</sup> (8 mm)</caption> <thead> <tr> <th>Pressure (bar)</th> <th>Blunt (J)</th> <th>Conical (J)</th> <th>Hemispherical (J)</th> </tr> </thead> <tbody> <tr> <td>15</td> <td>42</td> <td>45</td> <td>38</td> </tr> <tr> <td>20</td> <td>48</td> <td>45</td> <td>48</td> </tr> <tr> <td>25</td> <td>52</td> <td>45</td> <td>72</td> </tr> </tbody> </table>	Pressure (bar)	Blunt (J)	Conical (J)	Hemispherical (J)	15	42	45	38	20	48	45	48	25	52	45	72
Pressure (bar)	Blunt (J)	Conical (J)	Hemispherical (J)														
15	42	45	38														
20	48	45	48														
25	52	45	72														
Type E-800 g/m <sup>2</sup>	<p style="text-align: center;"><b>8 mm</b></p>  <table border="1" style="margin-left: auto; margin-right: auto;"> <caption>Data for Type E-800 g/m<sup>2</sup> (8 mm)</caption> <thead> <tr> <th>Pressure (bar)</th> <th>Blunt (J)</th> <th>Conical (J)</th> <th>Hemispherical (J)</th> </tr> </thead> <tbody> <tr> <td>15</td> <td>38</td> <td>42</td> <td>45</td> </tr> <tr> <td>20</td> <td>45</td> <td>45</td> <td>48</td> </tr> <tr> <td>25</td> <td>48</td> <td>48</td> <td>52</td> </tr> </tbody> </table>	Pressure (bar)	Blunt (J)	Conical (J)	Hemispherical (J)	15	38	42	45	20	45	45	48	25	48	48	52
Pressure (bar)	Blunt (J)	Conical (J)	Hemispherical (J)														
15	38	42	45														
20	45	45	48														
25	48	48	52														

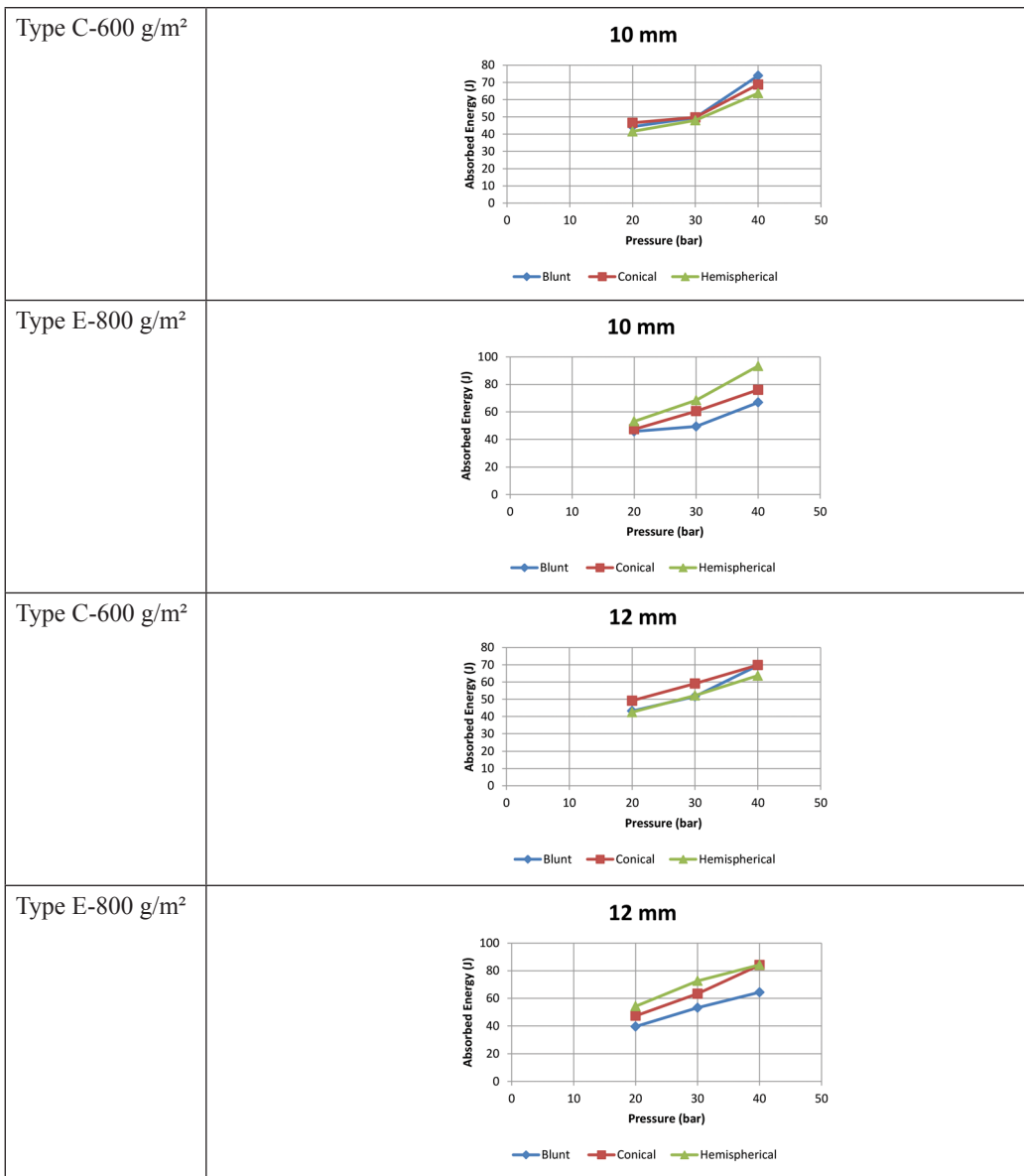


Figure 4. Absorbed Energy-Pressure curves for 6 mm, 8 mm, 10 mm and 12 mm thickness Type C-glass/epoxy 600 g/m<sup>2</sup> and Type E-glass/epoxy 800 g/m<sup>2</sup> composite panels

Figure 4 shows that as pressure increases, there is a corresponding increase in projectile velocity and absorbed energy. Increasing the initial velocity of the projectile makes penetration more localised, resulting in a proportional increase in the energy absorbed by the laminates. From the graphs, it can be seen that as the kinetic energy increased, the energy absorbed by the specimen also increased. The graphs also show that the conical projectile has the highest energy absorbed compared with hemispherical and blunt projectiles. The absorbed energy generated for impacts onto the Type E-800 g/m<sup>2</sup> are significantly larger than for Type C-600

g/m<sup>2</sup> due to its high stiffness. This shows that GFRP Type E-800 g/m<sup>2</sup> is stiffer than GFRP Type C-600 g/m<sup>2</sup>. It can be surmised that the greater the peak impact forces, the stiffer the projectile-to-target interactions. As projectile contact area decreases, energy absorption also increases. This results a greater damage made by the conical projectile during impact compared with the other two types of projectiles. Garcia-Castillo et al. (2013) noted two absorption mechanisms: energy absorbed by the tensile failure of the fibres, and the energy absorbed by the elastic deformation of the fibres.

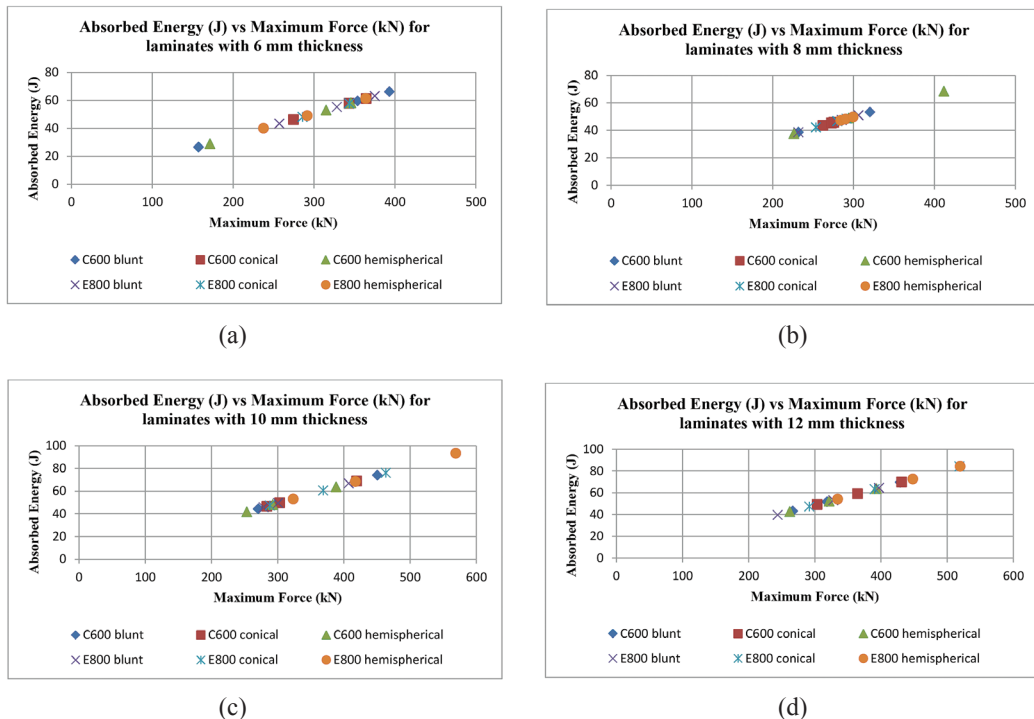


Figure 5. Absorbed Energy-Maximum Force curves for laminates (a) 6 mm (b) 8 mm (c) 10 mm (d) 12 mm thickness with Type C-Glass/Epoxy 600 g/m<sup>2</sup> and Type E-Glass/Epoxy 800 g/m<sup>2</sup>

Figure 5 shows the relationship between the maximum force and the absorbed energy for the GFRP Type C-600 g/m<sup>2</sup> and Type E-800 g/m<sup>2</sup> for the laminates with thickness of 6 mm, 8 mm, 10 mm and 12 mm. The graphs in Figure 5 show that the absorbed energy is directly proportional to the applied maximum force during impact. As the maximum force increases, there is corresponding increase in the value of the absorbed energy. This shows that maximum force has correlation with the energy absorbed. GFRP Type E-800 g/m<sup>2</sup> shows a higher maximum force compared with GFRP Type C-600 g/m<sup>2</sup> for all thicknesses as it has a greater impact resistance. The impact strength of a high impact resistant material is high thus greater force is needed to initiate damage. The laminate used in this experiment is a woven laminate. When no penetration of the laminates, the main energy-absorption mechanisms are fibre failure and elastic deformation. Therefore, the materials' initial stiffness and strength affect the impact behaviour of the laminates.

## CONCLUSION

This study has measured and evaluated the effects of impact profile on parameters such as the energy absorbed, maximum force, kinetic energy, and the initial velocity of projectiles. It was found that the gas gun pressure significantly increases the maximum force and kinetic energy, which means it has a direct correlation with the projectile impact velocity. The composite specimens with the highest thickness and density experienced the greatest impact energy absorption. As the gas gun pressure increases, the projectile kinetic energy, the projectile initial velocity and the maximum force exerted on the specimen also increases. All those increasing experimental parameters result in the proportional increases of the specimen energy absorption throughout the impact tests. The impact performances of GFRPs were mainly affected by specimen thickness, projectile shape and gas gun pressure. The laminates with Type E-800 g/m<sup>2</sup> are the strongest because of E-glass fibres are stronger compared with Type C 600 g/m<sup>2</sup>. The results show that GFRP with Type E-800 g/m<sup>2</sup> is better in terms of its impact performance in comparison with GFRP with Type C-600 g/m<sup>2</sup>, and this is due to E-glass fibre type's higher fibre volume and density together with its superior mechanical properties. Therefore, GFRPs with Type E-800 g/m<sup>2</sup> are recommended for future aircraft structural applications.

## ACKNOWLEDGEMENT

This work is supported by UPM under GP/IPB 9441503.

## REFERENCES

- Awerbuch, J., & Bodner, S. (1974). Analysis of the mechanics of perforation of projectiles in metallic plates. *International Journal of Solids And Structures*, 10(6), 671-684. <http://dx.doi.org/10.1016/0020-7683>
- Belingardi, G., & Vadori, R. (2002). Low velocity impact tests of laminate glass-fibre-epoxy matrix composite material plates. *International Journal of Impact Engineering*, 27(2), 213-229. [http://dx.doi.org/10.1016/s0734-743x\(01\)00040-9](http://dx.doi.org/10.1016/s0734-743x(01)00040-9)
- Bibo, G., & Hogg, P. (1998). Influence of reinforcement architecture on damage mechanisms and residual strength of glass-fibre/epoxy composite systems. *Composites Science And Technology*, 58(6), 803-813. [http://dx.doi.org/10.1016/s0266-3538\(97\)00055-9](http://dx.doi.org/10.1016/s0266-3538(97)00055-9)
- Børvik, T., Langseth, M., Hopperstad, O., & Malo, K. (2002). Perforation of 12mm thick steel plates by 20mm diameter projectiles with flat, hemispherical and conical noses. *International Journal of Impact Engineering*, 27(1), 19-35. <http://dx.doi.org/10.1016/s0734-743>
- Corran, R., Shadbolt, P., & Ruiz, C. (1983). Impact loading of plates — An experimental investigation. *International Journal of Impact Engineering*, 1(1), 3-22. <http://dx.doi.org/10.1016/0734>
- Davies, G., Hitchings, D., & Zhou, G. (1996). Impact damage and residual strengths of woven fabric glass/polyester laminates. *Composites Part A: Applied Science and Manufacturing*, 27(12), 1147-1156. [http://dx.doi.org/10.1016/1359-835x\(96\)00083-8](http://dx.doi.org/10.1016/1359-835x(96)00083-8)

- García-Castillo, S., Sánchez-Sáez, S., Santiuste, C., Navarro, C., & Barbero, E. (2013). Perforation of composite laminate subjected to dynamic loads. In S. Abrate, B. Castanié & Y. Rajapakse (Eds.), *Dynamic Failure of Composite and Sandwich Structures* (pp. 291-337). Springer Netherlands.
- Gellert, E., Cimpoeru, S., & Woodward, R. (2000). A study of the effect of target thickness on the ballistic perforation of glass-fibre-reinforced plastic composites. *International Journal of Impact Engineering*, 24(5), 445-456. [http://dx.doi.org/10.1016/s0734-743x\(99\)00175-x](http://dx.doi.org/10.1016/s0734-743x(99)00175-x)
- Grytten, F., Børvik, T., Hopperstad, O., & Langseth, M. (2009). Low velocity perforation of AA5083-H116 aluminium plates. *International Journal of Impact Engineering*, 36(4), 597-610. <http://dx.doi.org/10.1016/j.ijimpeng.2008.09.002>
- Hausrath, R., & Longobardo, A. (2010). High-strength glass fibres and markets. In F. Wallenberger & P. Bingham (Eds.), *Fibreglass and Glass Technology* (pp. 197-225). USA: Springer Science+Business Media.
- Ilcewicz, L., Cheng, L., Hafenricher, J., & Seaton, C. (2009). *Guidelines for the development of a critical composite maintenance and repair issues awareness course*. Washington: U.S. Department of Transportation.
- Mili, F. (2012). Effect of the Impact Velocity on the Dynamic Response of E-Glass/Epoxy Laminated Composites. *Arabian Journal for Science and Engineering*, 37(2), 413-419. <http://dx.doi.org/10.1007/s13369-012-0174-9>
- Naik, N., & Doshi, A. (2008). Ballistic impact behaviour of thick composites: Parametric studies. *Composite Structures*, 82(3), 447-464. <http://dx.doi.org/10.1016/j.compstruct.2007.01.025>
- Naik, N., & Shirao, P. (2004). Composite structures under ballistic impact. *Composite Structures*, 66(1-4), 579-590. <http://dx.doi.org/10.1016/j.compstruct.2004.03.026>
- Ohte, S., Yoshizawa, H., Chiba, N., & Shida, S. (1982). Impact Strength of Steel Plates Struck by Projectiles: Evaluation Formula for Critical Fracture Energy of Steel Plate. *Bulletin of JSME*, 25(206), 1226-1231. <http://dx.doi.org/10.1299/jsme1958.25.1226>
- Petrone, G., D'Alessandro, V., Franco, F., Mace, B., & De Rosa, S. (2014). Modal characterisation of recyclable foam sandwich panels. *Composite Structures*, 113, 362-368. <http://dx.doi.org/10.1016/j.compstruct.2014.03.026>
- Shaktivesh, N. N., Kumar, C. S., & Naik, N. (2013). Ballistic impact performance of composite targets. *Materials and Design*, 51, 833-846. <http://dx.doi.org/10.1016/j.matdes.2013.04.093>
- Sultan, M. H. (2007). *High velocity impact analysis of glass epoxy laminated plates*. (Master Dissertation). Universiti Putra Malaysia, Malaysia.
- Thanomsilp, C., & Hogg, P. (2003). Penetration impact resistance of hybrid composites based on commingled yarn fabrics. *Composites Science and Technology*, 63(3-4), 467-482. [http://dx.doi.org/10.1016/s0266-3538\(02\)00233-6](http://dx.doi.org/10.1016/s0266-3538(02)00233-6)
- Udatha, P., Kumar, C. S., Nair, N., & Naik, N. (2012). High velocity impact performance of three-dimensional woven composites. *The Journal of Strain Analysis For Engineering Design*, 47(7), 419-431. <http://dx.doi.org/10.1177/0309324712448578>
- Vaidya, U. (2011). Impact response of laminated and sandwich composites. In S. Abrate (Ed.), *Impact Engineering of Composite Structures* (pp. 97-191). New York: Springer Wien.

- Wen, H. (2000). Predicting the penetration and perforation of FRP laminates struck normally by projectiles with different nose shapes. *Composite Structures*, 49(3), 321-329. [http://dx.doi.org/10.1016/s0263-8223\(00\)00064-7](http://dx.doi.org/10.1016/s0263-8223(00)00064-7)
- Wen, H. (2001). Penetration and perforation of thick FRP laminates. *Composites Science and Technology*, 61(8), 1163-1172. [http://dx.doi.org/10.1016/s0266-3538\(01\)00020-3](http://dx.doi.org/10.1016/s0266-3538(01)00020-3)
- Zhou, G. (1995). Prediction of impact damage thresholds of glass fibre reinforced laminates. *Composite Structures*, 31(3), 185-193. [http://dx.doi.org/10.1016/0263-8223\(94\)00062-x](http://dx.doi.org/10.1016/0263-8223(94)00062-x)